On the Fading Parameters Characterization of the η-μ Distribution: Measurements and Statistics

Camila Lopes Selvati and Ugo Silva Dias

***Abstract*— This paper presents the results of field trial measurements in order to obtain the probability density functions and the cross-correlation functions of the fading parameters η and μ of the η-μ distribution. The ranges of possible practical values of the η and μ fading parameters are also obtained from the empirical data. In addition, the instantaneous magnitude variations of η and μ considering the mobile receiver displacement are estimated and discussed. The results provide important information about the practical usefulness of the η-μ fading model in mobile communication systems.**

***Keywords*— η-μ distribution, channel characterization, fading parameters, field measurements.**

***Resumo*— Este artigo apresenta os resultados de medições de campo com o objetivo de obter as funções densidade de probabilidade e as funções de correlação cruzada empíricas dos parâmetros de desvanecimento η e μ da distribuição η-μ. Os intervalos de possíveis valores práticos dos parâmetros de desvanecimento η e μ também são obtidos a partir dos dados adquiridos em campo. Ainda, as variações instantâneas de magnitude de η e de μ considerando o deslocamento do receptor móvel são estimadas e discutidas. Os resultados fornecem informações importantes sobre o uso prático do modelo de desvanecimento η-μ em sistemas de comunicações móveis.**

***Palavras-Chave*— Distribuição η-μ, caracterização de canal sem fio, parâmetros de desvanecimento, medições de campo.**

I. Introduction

THE phenomenon of multipath fading in wireless communications occurs when transmitted waves interact with the propagation medium producing partial waves with different amplitudes and phases. The combination of this signal fades rapidly and reaches the receiver through multiple paths. This behavior of the waves propagating in a mobile radio environment through multiple paths has been widely characterized by several well known statistical models, notably Rayleigh [1], Rice [2], [3], Hoyt (Nakagami-*q*) [4], [5], Nakagami-*m* [5], and Weibull [6]. More recently [7], a general physical fading model, namely the η-μ model, has been proposed which describes a signal composed of clusters of multipath waves propagating in a inhomogeneous environment. The η-μ distribution is written in terms of two measurable physical fading parameters η and μ. By setting specific values for η and μ, the η-μ fading model reduces to other important distributions such as Nakagami-*m* and Hoyt (Nakagami-*q*) [7]. (Therefore, One-Sided Gaussian and Rayleigh also constitute special cases of it.) Its flexibility renders it suitable to better fit field measurement data in a variety of scenarios [7]. Experimental data supporting the usefulness of the Nakagami-*m*, Hoyt, and Weibull fading models have been widely reported in the literature (e.g., [5], [8]–[12]). Recently [13]–[15], some works presenting the performance analysis and first-order statistical modeling for the Nakagami-*m* and Rice fading parameters have also been presented. In practice, situations are easily found for which the η-μ distribution outperforms both Nakagami-*m* and Hoyt [7], [16]. However, to the best of the authors' knowledge, works depicting practical situations in which the fading parameters of the η-μ distribution are characterized have not been reported in the literature.

In this paper, the empirical probability density functions (PDF) and the cross-correlation functions (CCF) of η and μ, which are the fading parameters of the η-μ distribution, are obtained based on field measurements. Furthermore, the ranges of possible practical values assumed by η and μ are estimated from the empirical data and their instantaneous magnitude variations are evaluated considering the displacement of the mobile receiver in outdoor environments. Since the values of η and μ are indicators of the scattered-wave components and multipath clustering of the radio channel [7], the knowledge of their PDFs, CCFs, and magnitude ranges can be used in the evaluation and design of different wireless communications techniques, such as diversity combining techniques, adaptive modulation schemes, modeling and analysis of interferences, outages probabilities, design and simulation of adaptive antennas systems, among others.

The remainder of this work is structured as follows. In Section II, the η-μ fading model is revisited. In Section III, field trial measurements are conducted in order to investigate first- and second-order statistics of the η and μ fading parameters. Specially, the empirical PDFs and CCFs of the η and μ fading parameters are presented and discussed based on the measurement campaigns. The instantaneous variation of the η and μ magnitudes are also obtained with distance and analyzed, and the practical value ranges of the η and μ parameters are estimated. Finally, in Section IV, some conclusion remarks are presented.

II. The η-μ Fading Model Revisited

The η-μ distribution is a general fading distribution that can be used to better represent the small-scale variation of the fading signal in a non-line-of-sight (NLOS) condition. It considers a signal composed of clusters of multipath waves propagating in a inhomogeneous environment. As its name implies, it is written in terms of two physical parameters,

The authors are with the Microwave and Wireless Systems Laboratory (MWSL), Department of Electrical Engineering, University of Brasilia, 70910-900, Brasília, DF, Brazil (e-mail: camilaselvati@ieee.org, udias@unb.br).

This work was partly supported by CNPq.

namely η and μ. It may appear in two different formats, hence two corresponding physical models are encountered [7]. One format can be obtained from another by the bilinear transformation $\eta_1 = \frac{1-\eta_2}{1+\eta_2}$ or, equivalently, $\eta_2 = \frac{1-\eta_1}{1+\eta_1}$, in which $0 < \eta_1 < \infty$ is the parameter η in Format 1, and $-1 < \eta_2 < 1$ is the parameter η in Format 2. So as to simplify the notation, η is used in both cases, bearing in mind that they represent different physical phenomena and their ranges are different.

For a η-μ fading signal with normalized envelope $\mathrm{P} = R/\hat{r}$ with $\hat{r} = \sqrt{E(R^2)}$ being the rms value of the envelope R, in which $E(\cdot)$ denotes the expectation operator, the η-μ envelope PDF, $f_{\mathrm{P}}(\rho)$, is written as [7]

$$f_{\mathrm{P}}(\rho) = \frac{4\sqrt{\pi}\mu^{\mu+\frac{1}{2}}h^{\mu}}{\Gamma(\mu)H^{\mu-\frac{1}{2}}}\rho^{2\mu}\exp\left(-2\mu h\rho^2\right)I_{\mu-\frac{1}{2}}\left(2\mu H\rho^2\right), \tag{1}$$

for which H and h will be defined next for each of the two formats of the model, $\Gamma(\cdot)$ is the Gamma function [17, Eq. 6.1.1], $I_\nu(\cdot)$ is the modified Bessel function of the first kind and order ν [17, Eq. 9.6.20], and $\mu > 0$ is given by

$$\mu = \frac{1}{2V(\mathrm{P}^2)}\left[1 + \left(\frac{H}{h}\right)^2\right], \tag{2}$$

with $V(\cdot)$ denoting the variance operator.

A. The η-μ Distribution: Format 1 and Format 2

In Format 1, the in-phase and quadrature components of the fading signal within each cluster are assumed to be independent from each other and to have different powers. $\eta > 0$ is the scattered-wave power ratio between the in-phase and quadrature components of each cluster of multipath and $\mu > 0$ is the number of multipath clusters. In such a case, $h = \frac{2+\eta^{-1}+\eta}{4}$ and $H = \frac{\eta^{-1}-\eta}{4}$, thus $H/h = (1-\eta)/(1+\eta)$. It is noted that for $0 < \eta \le 1$, $H \ge 0$, and for $0 < \eta^{-1} \le 1$, $H \le 0$. Because $I_\nu(-z) = (-1)^\nu I_\nu(z)$ the distribution yields identical values within these two intervals, i.e., it is symmetrical around $\eta = 1$. Therefore, as far as the envelope distribution is concerned, it suffices to consider η only within one of the ranges.

In Format 2, the in-phase and quadrature components of the fading signal within each cluster are assumed to have identical powers and to be correlated with each other. $-1 < \eta < 1$ is the correlation coefficient between the scattered-waves in-phase and quadrature components of each cluster of multipath and $\mu > 0$ is the number of multipath clusters. In such a case, $h = \frac{1}{1-\eta^2}$ and $H = \frac{\eta}{1-\eta^2}$, thus $H/h = \eta$. It is noted that for $0 \le \eta < 1$, $H \ge 0$, and for $-1 < \eta \le 0$, $H \le 0$. Because $I_\nu(-z) = (-1)^\nu I_\nu(z)$ the distribution yields identical values within these two intervals, i.e., it is symmetrical around $\eta = 0$. Therefore, as far as the envelope distribution is concerned, it suffices to consider η only within one of the ranges.

B. Obtaining the Traditional Fading Models

Interestingly, by setting some specific values for the fading parameters η and μ, the η-μ distribution reduces to traditional models. For $\mu = 0.5$, the η-μ distribution reduces to the Hoyt (Nakagami-*q*) distribution. In this case, the Hoyt (Nakagami-*q*) fading parameter is given by $b = -\frac{1-\eta}{1+\eta}$ (or $q^2 = \eta$) in Format 1 or $b = -\eta$ (or $q^2 = \frac{1-\eta}{1+\eta}$) in Format 2. The Nakagami-*m* distribution can be obtained from the η-μ distribution by setting $\mu = m$ and $\eta \to 0$ or $\eta \to \infty$ in Format 1, or $\eta \to \pm 1$ in Format 2. In the same way, it can be obtained by setting $\mu = m/2$ and $\eta \to 1$ in Format 1 or $\eta \to 0$ in Format 2. The One-Sided Gaussian distribution can be also obtained by setting $\eta \to 0$ or $\eta \to \infty$ in Format 1, or $\eta \to \pm 1$ in Format 2. In the same way, the Rayleigh distribution is obtained in an exact manner for $\mu = 0.5$ and by setting $\eta = 1$ in Format 1 or $\eta = 0$ in Format 2.

III. Field Trials and Statistical Analysis

A series of field trials was conducted at the University of Campinas (Unicamp), Brazil, in order to (i) estimate the value ranges of the η and μ parameters, (ii) characterize the amplitude variations with distance of the η and μ fading parameters, (iii) obtain the empirical PDFs of the η and μ parameters, and (iv) obtain the empirical CCFs of such fading parameters. To this end, the transmitter was placed on the rooftop of one of the buildings as can be seen in Figure 1, and the receiver traveled through and outside the campus with a constant speed of 30 km/h. Figures 2 to 4 present some outdoor environments where the mobile receiver was displaced during the measurement campaigns. Note the variety of physical characteristics present in these scenarios, such as, trees, parked and moving cars, people, and buildings with different numbers of floors, constituting typical suburban and urban areas. The mobile reception equipment was especially assembled for this purpose. Basically, the setup consisted of a vertically polarized omnidirectional receiving antenna, a low noise amplifier, a spectrum analyzer, data acquisition apparatus, a notebook computer, and a distance transducer for carrying out the signal sampling. The transmission consisted of a continuous wave tone at 5.5 GHz. The spectrum analyzer was set to zero span and centered at the desired frequency, and its output used as the input of the data acquisition equipment with a sampling interval of $\lambda/180$ [18], [19]. The local mean was estimated by the moving average method, with the average being conveniently taken over samples symmetrically adjacent to every point. From the collected data, the long term fading was filtered out, then the η and μ fading parameters could be estimated using the following moment-based estimator.

A. The Moment-based η-μ Estimator

The jth moment, $E(\mathrm{P}^j)$, of P, is given as [7]

$$E(\mathrm{P}^j) = \frac{\Gamma(2\mu + j/2)}{h^{\mu+j/2}(2\mu)^2\Gamma(2\mu)} \times {}_2F_1\left(\mu + \frac{j}{4} + \frac{1}{2}, \mu + \frac{j}{4}; \mu + \frac{1}{2}; \left(\frac{H}{h}\right)^2\right), \tag{3}$$

in which ${}_2F_1(\cdot,\cdot;\cdot;\cdot)$ is the Gauss hypergeometric function [17, Eq. 15.1.1] and $E(R^j) = \hat{r}^j E(\mathrm{P}^j)$. Replacing (2) in (3) an equality is defined that is useful for the estimation of the η parameter of this distribution. Note that for a given value of

Fig. 1. Building 'E' – Faculty of Electrical and Computing Engineering. Transmitter on the rooftop.

Fig. 2. Antonio Augusto Almeida Street. Outdoor measurements. NLOS condition.

Fig. 3. Professor Atilio Martins Avenue. Outdoor measurements. NLOS condition.

Fig. 4. Cora Coralina Street. Outdoor measurements. NLOS condition.

j, the physical parameter η is encountered and then μ can be found from Eq. (2). In [7], closed-form formulations for the determination of η [7, Eq. 28] and μ are obtained for $j = 6$. However, such formulations are not able to estimate positive real values for η and μ in almost all of our measurement data. Thus, in this work, it is necessary to decrease the power value of P by setting $j = 3$ in order to obtain non-complex positive values of η and μ. Note that from (3) several moment-based estimators can be found.

B. The Empirical Cross-correlation

The normalized empirical CCF was computed according to

$$\widehat{R}_{R_1,R_2}(\Delta) = \frac{\sum_{i=1}^{N-\Delta} r_{1_i} r_{2_{i+\Delta}}}{\sum_{i=1}^{N-\Delta} r_{1_i} r_{2_i}} \tag{4}$$

in which r_{1_i} and r_{2_i} are the i-th samples of the amplitude sequences of R_1 and R_2, respectively, N is the total number of samples, Δ is the discrete relative distance difference, and $\widehat{R}_{R_1,R_2}(\cdot)$ denotes an empirical estimate of $R_{R_1,R_2}(\cdot)$.

C. Numerical Results and Discussion

Figures 5 to 7 show sample plots of the magnitude variations of the η and μ fading parameters with distance, which are represented by the outdoor environments with NLOS conditions of Figures 2 to 4, respectively. In such cases and in all of our measurement data, we consider the Format 1 to compute the η and μ fading parameters. It can be noted that η increases and μ decreases when $0 < \eta < 1$. For $\eta > 1$, μ increases whenever η increases. These interesting behaviors of the two fading parameters, as predicted by their theoretical model [7] are now confirmed in practice.

Figures 8, 9, and 10 present the fitting between the theoretical PDF of the η-μ distribution and the empirical PDFs of the η and μ fading parameters, for the same environments of the Figures 5, 6 and 7, respectively. Note that the PDFs of both η and μ have similar shapes, but they are centered in different values and they seem to approximately follow a positive gaussian PDF. The values that η assume for which the η-μ theoretical PDF fits to the empirical PDFs of η vary from 3.54 to 4, and μ varies from 1.82 to 3.2. The η-μ theoretical PDF fits to the empirical PDFs of μ when $\eta = 2$ and μ varies from 2 to 2.3. The average estimated median and mean values of η, considering all measurement data, are respectively 1.73 and 1.89, with standard deviations of 0.60. For the μ cases, these are respectively 0.58 and 0.59, with standard deviations of 0.04. The range of possible practical values of η, as found here, vary from 0.9 to 3.9. And for the μ case, these are from 0.5 to 0.7. The knowledge of possible practical levels of η and μ and their expected values is very important to better estimate the fading margin in wireless systems.

Finally, Figures 11, 12, and 13 depict sample plots of the empirical CCF of the η and μ fading parameters for different outdoor environments. Interestingly, observe how the η and μ curves tend to keep track of the changes of the concavity of each other with slight shifts.

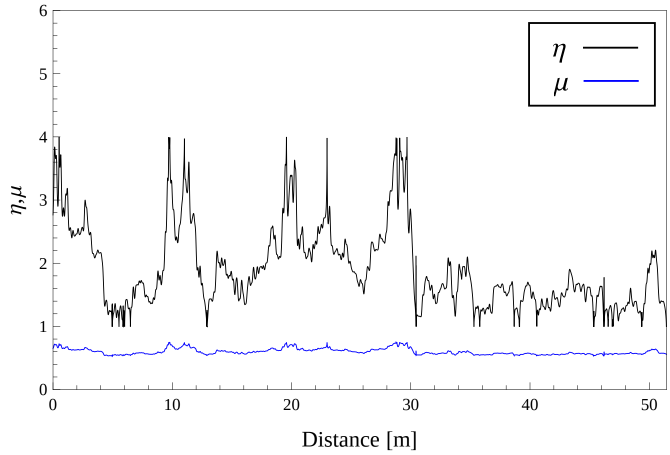

Fig. 5. η and μ magnitudes with distance. Outdoor measurements in NLOS conditions.

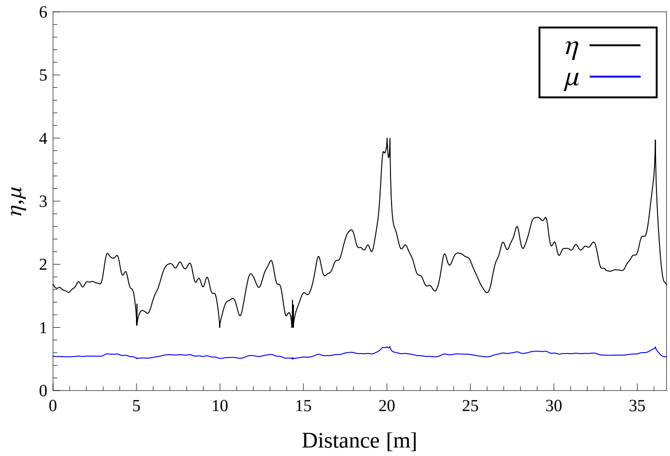

Fig. 6. η and μ magnitudes with distance. Outdoor measurements in NLOS conditions.

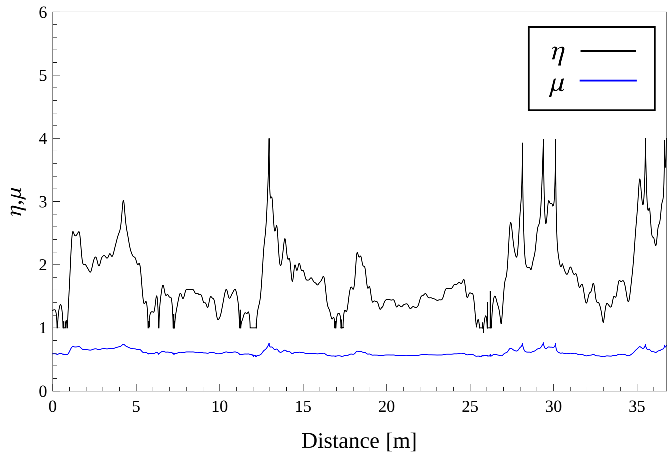

Fig. 7. η and μ magnitudes with distance. Outdoor measurements in NLOS conditions.

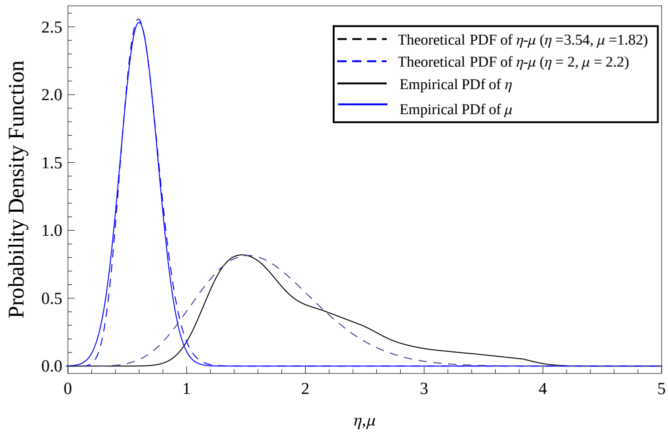

Fig. 8. Empirical PDFs of the η and μ fading parameters being fitted by the theoretical PDFs of the η-μ distribution.

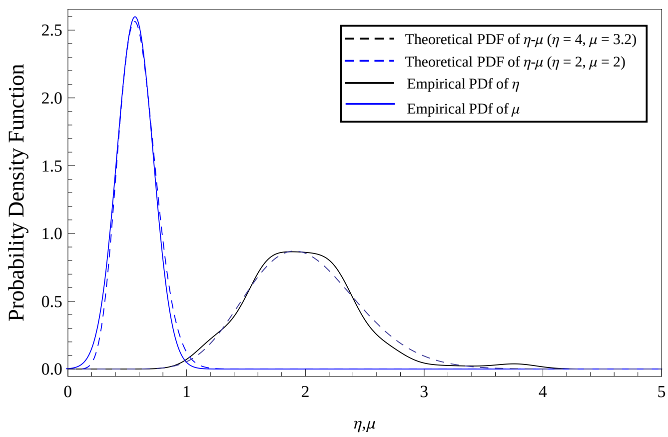

Fig. 9. Empirical PDFs of the η and μ fading parameters being fitted by the theoretical PDFs of the η-μ distribution.

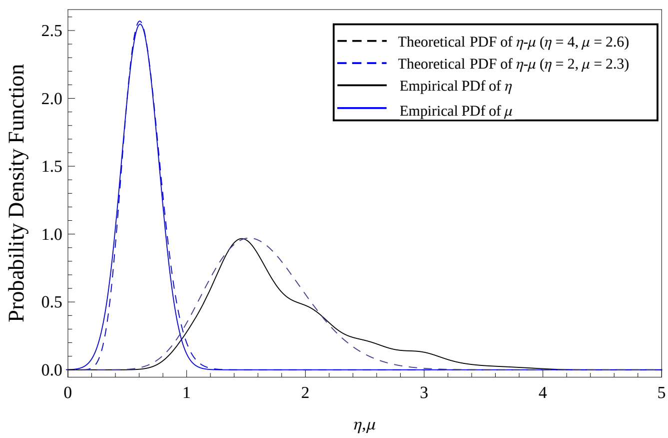

Fig. 10. Empirical PDFs of the η and μ fading parameters being fitted by the theoretical PDFs of the η-μ distribution.

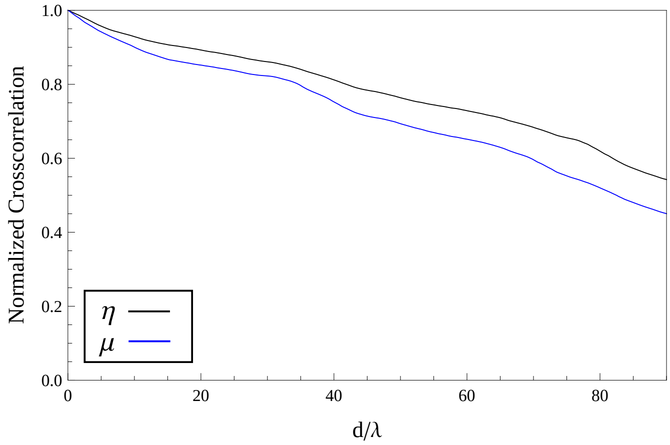

Fig. 11. Empirical CCFs of the η and μ fading parameters. Outdoor measurements in NLOS conditions.

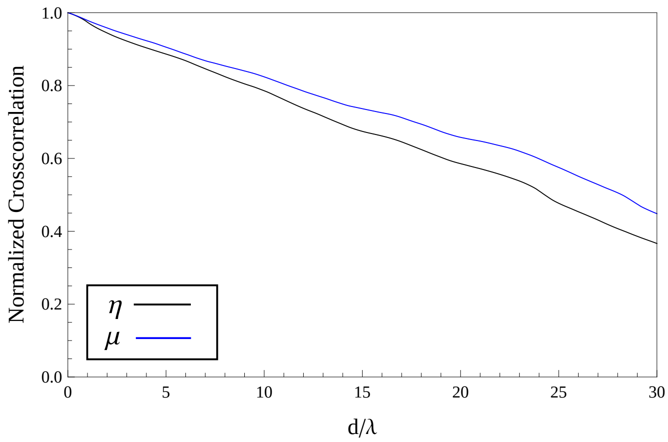

Fig. 12. Empirical CCFs of the η and μ fading parameters. Outdoor measurements in NLOS conditions.

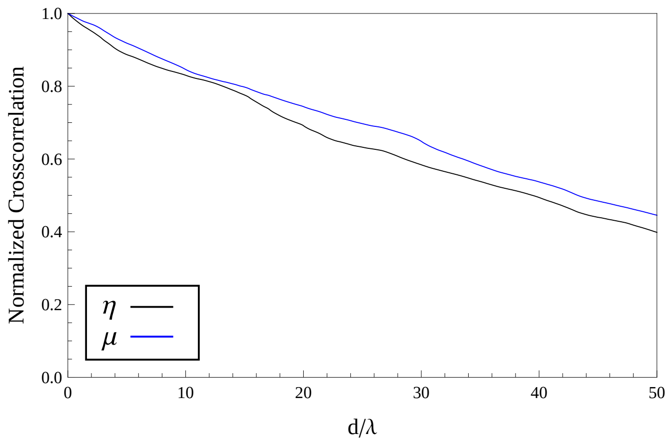

Fig. 13. Empirical CCFs of the η and μ fading parameters. Outdoor measurements in NLOS conditions.

IV. Conclusions

In this paper, we reported the results of field trials aimed at investigating first- and second-order statistics of the fading parameters of the η-μ distribution. More specifically, the empirical probability density functions and the cross-correlation functions of the η and μ fading parameters were obtained. Moreover, the ranges of possible practical values for the η and μ fading parameters were estimated from the empirical data, and the instantaneous variations of their magnitudes were evaluated considering the displacement of the mobile receiver in outdoor environments. The results provided important information about the practical usefulness of the η-μ fading model in mobile communication systems.

References

[1] R. H. Clarke, "A statistical theory of mobile-radio reception," *Bell Syst. Tech. J.*, vol. 47, pp. 957–1000, Jul.–Aug. 1968.

[2] S. O. Rice, "Mathematical analysis of random noise," *Bell Syst. Tech. J.*, vol. 23, no. 3, pp. 282–332, Jul. 1944.

[3] ——, "Mathematical analysis of random noise," *Bell Syst. Tech. J.*, vol. 24, no. 1, pp. 46–156, Jan. 1945.

[4] R. S. Hoyt, "Probability functions for the modulus and angle of the normal complex variate," *Bell Syst. Tech. J.*, vol. 26, pp. 318–359, Apr. 1947.

[5] M. Nakagami, *The m-Distribution – a general formula of intensity of rapid fading*. Statistical Methods in Radio Wave Propagation, Permagon Press, 1960.

[6] M. D. Yacoub, D. B. da Costa, U. S. Dias, and G. Fraidenraich, "Joint Statistics for Two Correlated Weibull Variates." *IEEE Ant. and Wireless Prop. Lett.*, vol. 4, pp. 129–132, May 2005.

[7] M. D. Yacoub, "The κ-μ and the η-μ distribution," *IEEE Antennas Propag. Mag.*, vol. 49, no. 1, pp. 68–81, Feb. 2007.

[8] U. S. Dias, M. D. Yacoub, J. C. S. Santos Filho, G. Fraidenraich, and D. B. da Costa, "On the Nakagami-*m* Autocorrelation and Power Spectrum Functions: Field Trials and Validation," in *IEEE International Telecommunications Symposium, ITS'06*, Fortaleza-CE, Brazil, Sep. 2006, pp. 253–256.

[9] N. Youssef, C.-X. Wang, and M. Patzold, "A study on the second order statistics of nakagami-hoyt mobile fading channels," *IEEE Transactions on Vehicular Technology*, vol. 54, no. 4, pp. 1259 – 1265, july 2005.

[10] H. Hashemi, "The indoor radio propagation channel," *Proc. IEEE*, vol. 81, pp. 943–968, Jul. 1993.

[11] G. Tzeremes and C. G. Christodoulou, "Use of Weibull distribution for describing outdoor multipath fading," in *Proc. IEEE Antennas and Propagation Soc. Int. Symp.*, vol. 1, Jun. 2002, pp. 232–235.

[12] F. Babich and G. Lombardi, "Statistical analysis and characterization of the indoor propagation channel," *IEEE Trans. Commun.*, vol. 48, pp. 455–464, Mar. 2000.

[13] L. Rubio, J. Reig, and N. Cardona, "Evaluation of nakagami fading behaviour based on measurements in urban scenarios," *AEU - International Journal of Electronics and Communications*, vol. 61, no. 2, pp. 135 – 138, 2007.

[14] L. Greenstein, S. Ghassemzadeh, V. Erceg, and D. Michelson, "Ricean K-Factors in Narrow-Band Fixed Wireless Channels: Theory, Experiments, and Statistical Models," *IEEE Transactions on Vehicular Technology*, vol. 58, no. 8, pp. 4000 –4012, oct. 2009.

[15] C. Oestges, B. Villacieros, and D. Vanhoenacker-Janvier, "Radio Channel Characterization for Moderate Antenna Heights in Forest Areas," *IEEE Transactions on Vehicular Technology*, vol. 58, no. 8, pp. 4031 –4035, oct. 2009.

[16] H. B. Tercius, *Generalized short-term fading distributions: field measurements and validations*. Ph.D. dissertation, University of Campinas, 2008.

[17] M. Abramowitz and I. A. Stegun, *Handbook of Mathematical Functions with Formulas, Graphs, and Mathematical Tables*. New York: Dover, 1972.

[18] B. Davis, and R. Bogner, "Propagation at 500 MHz for mobile radio," *IEEE Proc.*, vol. 132, Aug. 1985.

[19] K. T. .J. Horikoshi and T. Morinaga, "1.2 GHz Band Wave Propagation Measurements in Concrete Buildings for Indoor Radio Communication," *IEEE Trans. Veh. Tech.*, vol. 35, Aug. 1986.